J Mater Sci: Mater Electron (2015) 26:6004–6012
DOI 10.1007/s10854-015-3176-z

Effects of titanium on active bonding between Sn3.5Ag4Ti(Ce,Ga) alloy filler and alumina

L. X. Cheng[1] · G. Y. Li[1] · Z. L. Li[1] · Z. Z. Wu[1] · B. Zhou[2]

Received: 1 February 2015 / Accepted: 5 May 2015 / Published online: 12 May 2015

Abstract The role of active element titanium for the bonding alumina substrates using Sn3.5Ag4Ti(Ce,Ga) alloy filler at 250 °C in air was studied. The influence of soldering time on the microstructure and element distribution was investigated. It was observed that the Sn3.5Ag4Ti(Ce,Ga) solder could wet the alumina well under the agitation of external force. No continuous reaction products could be detected at the alumina/solder interface by using scanning electron microscopy and X-ray diffractometer. It might be inferred that the joining could be accomplished by chemical adsorption of Ti on the alumina/solder interface, regardless of whether or not an interfacial reaction layer is formed. The theoretical analysis of the Ti element adsorption at the alumina/solder interface was tried. Results can further explain the adsorption phenomenon of Ti at the interface prior to bond formation. In the case of environmental temperature has yet to meet the chemical reaction conditions, the chemical adsorption between active elements and alumina can get good bond as well. The shear strengths of the soldered Al_2O_3/Al_2O_3 substrates with the soldering time of 15 min, 30 min, and 1 h were measured to be 15.46, 16.15, and 17.39 MPa respectively.

✉ G. Y. Li
phgyli@scut.edu.cn

[1] School of Electronic and Information Engineering, South China University of Technology, Guangzhou 510641, China

[2] Science and Technology on Reliability Physics and Application Technology of Electronic Component Laboratory, Guangzhou 510610, China

1 Introduction

In the integrated circuit package, new package materials such as aluminum oxide, silicon carbide, beryllium oxide and so on are more and more widely used. Due to their unique electronic, chemical, mechanical, and physical properties, there is a good application for them as encapsulation substrate in discrete semiconductor devices, integrated circuits, hybrid circuit, and high performance packages.

Nowadays, among many Pb-free solders, SnAgCu alloy system has been regarded as a promising candidate due to the merit of high strength, longer thermal fatigue life, good creep resistance, and low cost [1]. Although this alloy system shows a satisfactory wettability and solderability with many metallic substrates, it cannot be used for the bonding of ceramic materials without pre-metallization. Active welding possesses a major advantage compared with conventional welding, as the base materials do not need pre-metallization. Traditionally, a key component in the design of welding alloys for ceramic joining is the addition of reactive elements such as Ti, Cr, Zr, etc. [2] to enhance the activity. However, the interfacial thermal stress generated due to the difference in thermal-expansion coefficients of the ceramic and metal during the cooling process after welding might deteriorate the joints [3, 4]. To solve this problem, low melting-point Sn base active fillers have been developed, as the melting-point of the Sn base solder is the lowest among all the solders.

In many previous studies [5, 6], it can be found that adding Ti element can make the best performance of the active solder, both for the improvement of the wettability and mechanical properties. However, most of the work with active solder added Ti element concentrated upon high temperature solder AgCuTi [3, 7–9]. And very little

Table 1 Composition of the active solder

Element	Sn	Ag	Ti	Other active elements (Ga, Ce)
wt%	91.5–93.5	3.5–4.0	3.1–4.1	0.0–0.2

papers discussed the performance of low temperature active solder. Especially for SnAgTi solder, only Chang and Koleňák etc. conducted research on it. Chang [10] only took some simple observation of the interface microstructure and performed tests on the mechanical properties of the joints. Koleňák [11] only performed tests on the mechanical strength of the joints fabricated by ultrasonic activation in air, did not analyze the micro interface. So it is necessary to take in-depth research and analysis on the soldering alumina by SnAgTi filler. In addition, it is unproven that whether compound formation at the interface between alumina and solder is actually necessary for the completion of joining. Okamoto et al. indicated in a review paper that interfacial reactions are unavoidable in most metal-ceramic joining. The formation of interfacial structures and morphologies affects the wetting process and the joining strength of brazed ceramic components. However, Chung [12], Gremillard [13] and Kalogeropoulou [14] demonstrated that joining could be accomplished by chemical adsorption of Ti at the interface, regardless of whether or not an interfacial reaction layer was formed. To well understand the soldering mechanisms of low temperature active solder with alumina, the soldering processes of Sn3.5Ag4Ti (Ce,Ga) and alumina at low temperature in air, the microstructure analysis of the interface, and the evolution of Ti element distribution for different soldering times have been investigated in this study. The bonding strengths have been measured for the samples in different soldering time and the shear fracture microstructure has been analyzed.

2 Experimental

The active solder Sn3.5Ag4Ti (Ce,Ga) used in this study was supplied by S-BOND Technologies and its composition is listed in Table 1. The solidus and liquidus temperatures of the solder are 221 and 232 °C respectively. The alumina for joining used in this study, 95 % Al_2O_3, was sliced into 10 mm × 10 mm and 5 mm × 5 mm as the bonding substrate. The bonding surfaces of the alumina specimens were wet ground with SiC paper of grade 600 first, and then down to grade 2000. The alumina and the active filler alloy were ultrasonic cleaned in alcohol, acetone and deionized water for 5 min each, and then dried in nitrogen at room temperature. Prior to soldering, the alumina specimens were preheated on a heating plate at 250 °C for 5 min. The active alloy filler was then placed on the bond surface. Once the alloy was molten, the molten alloy was agitated for about 30 s for wetting on the bond surface, and then another alumina specimen was placed on the molten solder to be joined by being rubbed together for 30 s. The joint was held firmly in place and cooled, leading to the solidification of the molten solder.

The schematic representation of soldering is demonstrated in Fig. 1. As enhanced bond strength and a superior joint seal can be obtained with longer soldering time based on the information from S-Bond Technologies, the soldering time were set to be 15, 30, and 60 min respectively at 250 °C. For the metallographic observation, the samples were prepared with their cross sections by conversional metallographic procedures. The microstructures and element distribution were analyzed by a scanning electron microscopy (HITACHI S-3700 N) coupled with energy dispersive spectrometer (EDS). X-ray diffractemeter (Bruker D8 ADVANCE) was used to detect intermetallic phases formed at the bonding interfaces, to ascertain the bonding mechanism and related interfacial reactions. The bonding strengths were measured by shear testing which was performed with a bond tester (MFM1500) according to MIL-STD-883G-2006. The geometry and dimensions of the soldering specimens subjected to shear testing are demonstrated in Fig. 2. The shear strengths were determined by averaging the test values of 10 samples for each test sample group. Fractured surfaces were observed by using scanning electron microscopy (SEM) and the residuals on the fracture surfaces were analyzed by EDS.

3 Results and discussion

3.1 Microstructure

The interfacial microstructure and element maps of Al_2O_3/Sn3.5Ag4Ti(Ce,Ga)/Al_2O_3 joint soldered at 250 °C for 15 min are shown in Fig. 3. EDS analysis shows that Ti

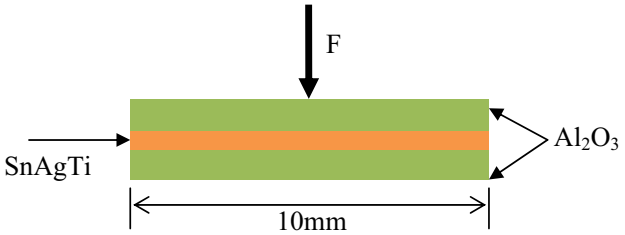

Fig. 1 Schematic representation of soldering

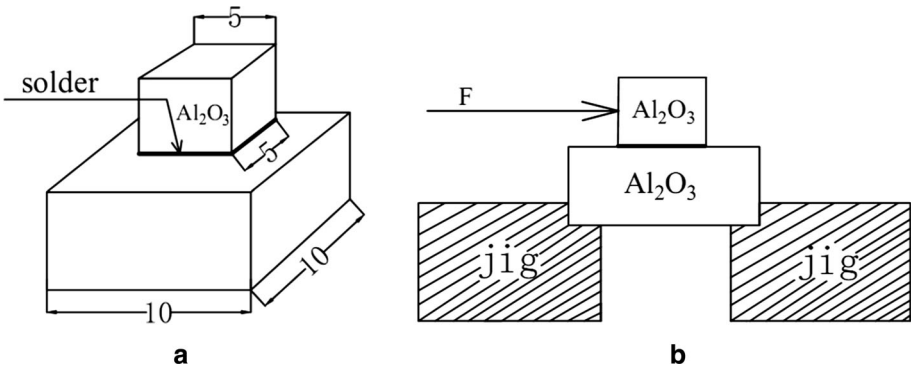

Fig. 2 Schematic representation for shear testing (Units: mm)

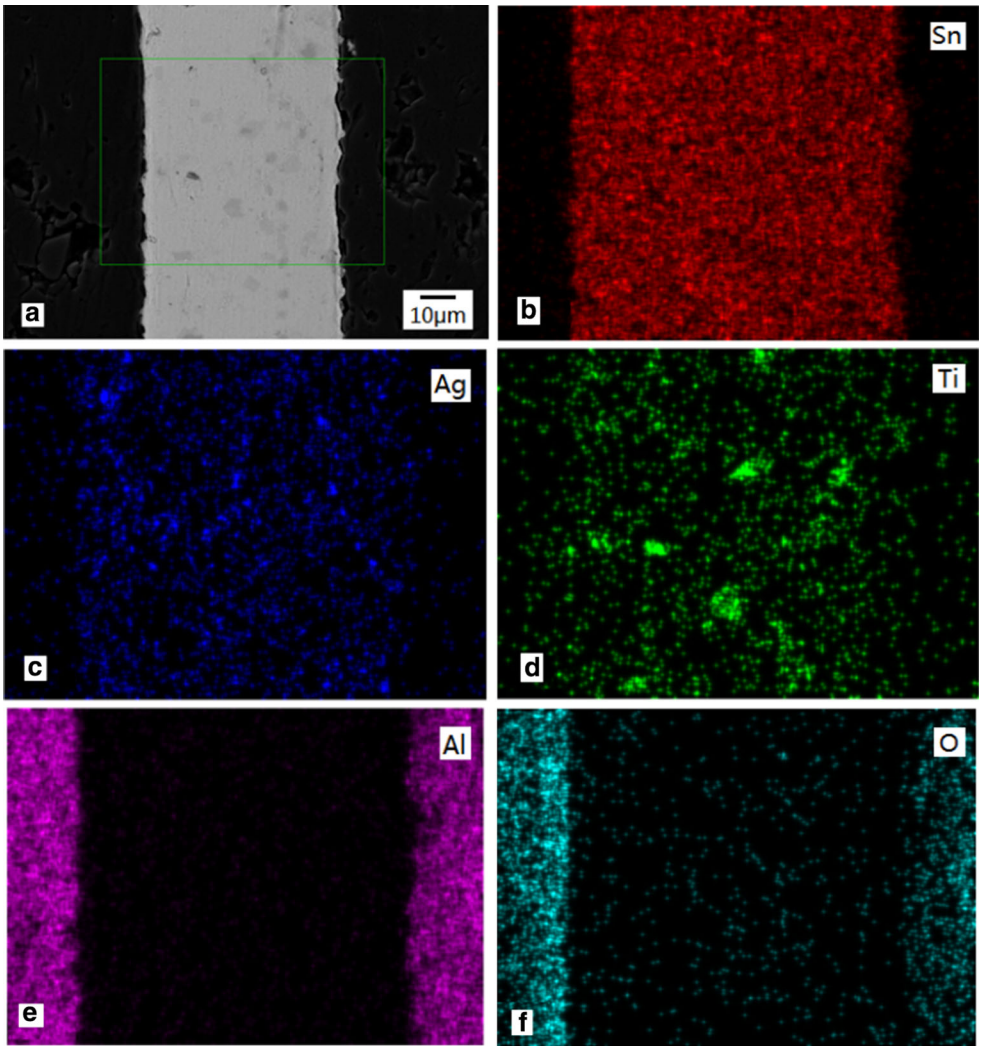

Fig. 3 Micrograph and element maps for Al_2O_3/Sn3.5Ag4Ti(Ce,Ga)/Al_2O_3 joint soldered at 250 °C for 15 min **a** micrograph; **b** map of tin; **c** map of silver; **d** map of titanium; **e** map of aluminum; **f** map of oxygen

element clusters together inside the Sn3.5Ag4Ti(Ce,Ga) filler metal after soldering, as shown in Fig. 3d. Titanium is not found to obviously segregate at the alumina/active solder interface. The element maps of the tin, silver, aluminum, and oxygen are shown in Fig. 3b, c, e, and f respectively.

Microstructure and element maps of Al_2O_3/Sn3.5Ag4 Ti(Ce,Ga)/Al_2O_3 joint soldered at 250 °C for 30 min are

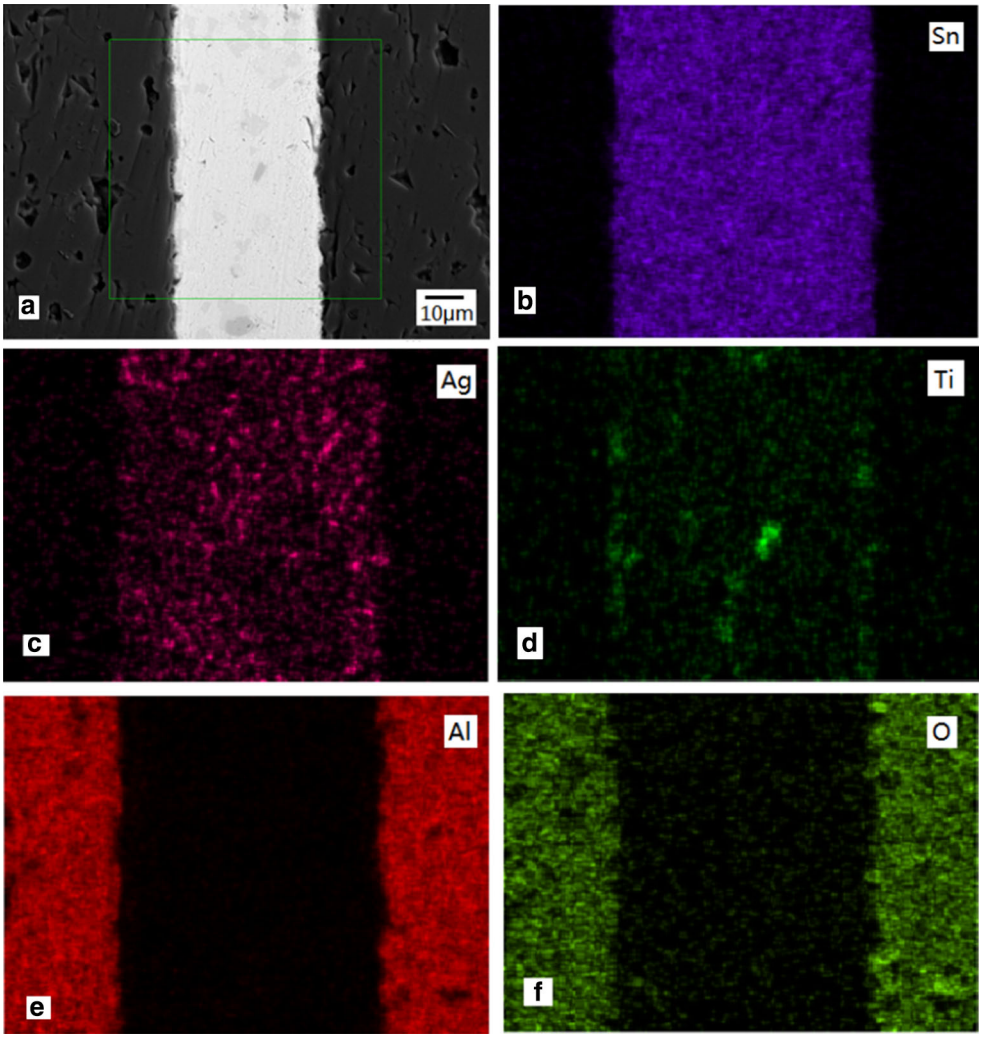

Fig. 4 Micrograph and element maps for Al_2O_3/Sn3.5Ag4Ti(Ce,Ga)/Al_2O_3 joint soldered at 250 °C for 30 min **a** micrograph; **b** map of tin; **c** map of silver; **d** map of titanium; **e** map of aluminum; **f** map of oxygen

shown in Fig. 4. EDS analysis shows that titanium obviously segregates at the alumina/active solder interface, as shown in Fig. 4d. A line scan was also performed to detect titanium across the interface, as shown in Fig. 5. It can be found that a peak of relative titanium concentration is appeared at the interface, which further confirms that titanium segregates at the alumina/active solder interface.

Microstructure and element maps of Al_2O_3/Sn3.5Ag4 Ti(Ce,Ga)/Al_2O_3 joint soldered at 250 °C for 60 min are shown in Fig. 6. EDS analysis shows that segregation of titanium at the alumina/active solder interface become not obvious, as shown in Fig. 6d, which is totally different from Fig. 4d, and titanium element almost uniformly distributes inside the solder.

XRD analysis performed at the fracture interface of the alumina/active solder after mechanical separation is shown in Fig. 7. Results show that there is no reaction phase formed at the interface. To well understand the reason why no reaction phases are formed, it is necessary to take in-depth research and analysis from the perspective of thermodynamics.

The thermodynamic feasibility of any reaction at a particular temperature can be determined by calculating the free energy change for the reaction at that particular temperature. In our material system, the chemical reaction between the active element in Sn–Ag–Ti filler alloy, i.e. Ti, and the ceramic substrate, may promote the soldering successfully as follows [15],

$$Al_2O_3(s) + 3Ti(l) = 3TiO(s) + 2Al(l) \quad (1)$$

Under the soldering atmosphere the pressure is kept constant, thus the feasibility of the above reaction at different soldering temperature can be calculated using Gibb's–Helmholtz equation, i.e.

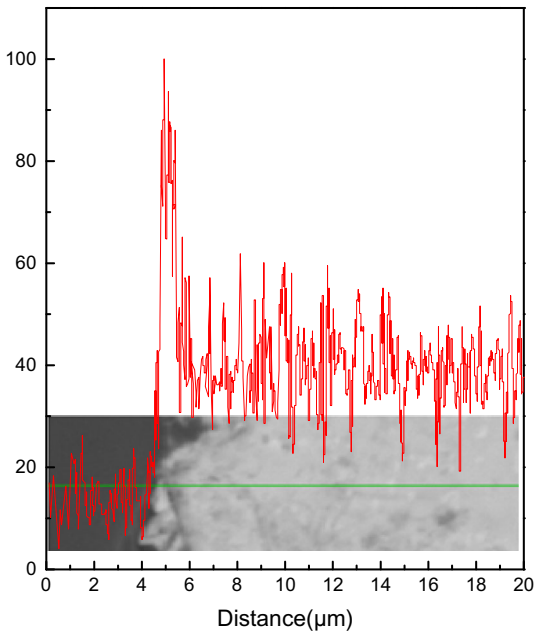

Fig. 5 Line scan of Ti for Al_2O_3/Sn3.5Ag4Ti(Ce,Ga)/Al_2O_3 joint welding at 250 °C for 30 min

$$\Delta G_T = \Delta H_T - T\Delta S \quad (2)$$

The relevant thermodynamic data for the formation of TiO during soldering are tabulated in Table 2 [15]. From Table 2, it can be found that the equilibrium temperature for the formation of TiO is 1209.21 K, and the reaction is thermodynamically feasible above this temperature. In the present study the sample was soldered at 250 °C that is much lower than the equilibrium temperature. Then, it is impossible to take any reaction in terms of thermodynamics. This may be the reason why no reaction products were observed at the interface.

3.2 The dynamic processes of soldering

This experiment was operated in atmospheric environment, and the oxide layer could be formed [16] to prevent the molten solder spreading out on alumina surface. As a consequence, different from other soldering processes, it is necessary to use external force to destroy the surface oxidation film of the molten solder. In the process of agitation about 30 s in this experiment, liquid surface oxidation film can be damaged by the external force. Hence the liquid can spread out in a very short time and the molten solder can wet alumina substrate very well in the experiment.

To well understand the soldering mechanisms of low temperature active solder with alumina, it is necessary to explore the soldering processes. In the molten active solder, the movement of an active atom in a large amount of liquid group atoms is actually a complex micro process including a continuous collision, rebound, complexation, and dissociation. Whether or not the selective adsorption of the active atoms on the solid–liquid interface takes place, it mainly depends on the interaction between the active atoms and the solvent atoms. In the molten solder, there is a repulsive force between the dissolved active atoms and tin atoms [17]. Presumably, it is this repulsive force, some of the titanium atoms may be squeezed out onto the liquid surface and the solid–liquid interface, some may return to the interface of clustered particles. Based on the above analysis, through a long distant migration, the last active elements will have two existing status: occupy the liquid surface and solid–liquid interface, and cluster inside of the liquid. This is consistent with the observation in our study that Ti element can cluster together inside the Sn3.5Ag4Ti (Ce,Ga) filler metal after soldering, as shown in Figs. 3d, 4d, and 5d.

There are two possible ways by which an active atom in a spreading droplet may move to the liquid–solid interface [17]. The first is to pass directly from the droplet to the interface by Brownian motion. The active atom, after innumerable collisions with other atoms, may ultimately reach the solid–liquid interface. If the attractive force of the solid surface to the active atom is stronger than that of the liquid body, the active atom would remain on the interface. The second way is indirect. The active atom first reaches and stays at the surface of the liquid by Brownian motion, then continues to move to the solid–liquid interface from the liquid surface. In both ways the most important factors are the segregating ability of the active atoms in the liquid and the strength of the attraction of the solid surface to the active atom [17].

In the initial stage of soldering, according to the model of Dussan–Davis movement [18, 19] as shown in Fig. 8, the active atoms segregated on liquid surface could easily move to the solid–liquid interface. The driving force of the Dussan–Davis movement which transfers surface atoms to the solid–liquid interface should come from the adsorption of the active atoms on the solid–liquid interface.

In the second stage of soldering, when two pieces of alumina substrate lay in sandwich structure in the atmosphere under a certain force, the way which active atoms transport through liquid surface to the solid–liquid interface is basically interrupted. There is only the first way that is possible to make active atoms continue to move to solid–liquid interface. Assuming that the transport speed of active atoms is faster than the speed of active atoms being consumed at the interface, a temporary stack of active atoms at the interface may occur. On the contrary, assuming that the transport speed of active atoms is slower than the speed of active atoms being consumed at the interface, a temporary stack of active atoms at the interface may not occur.

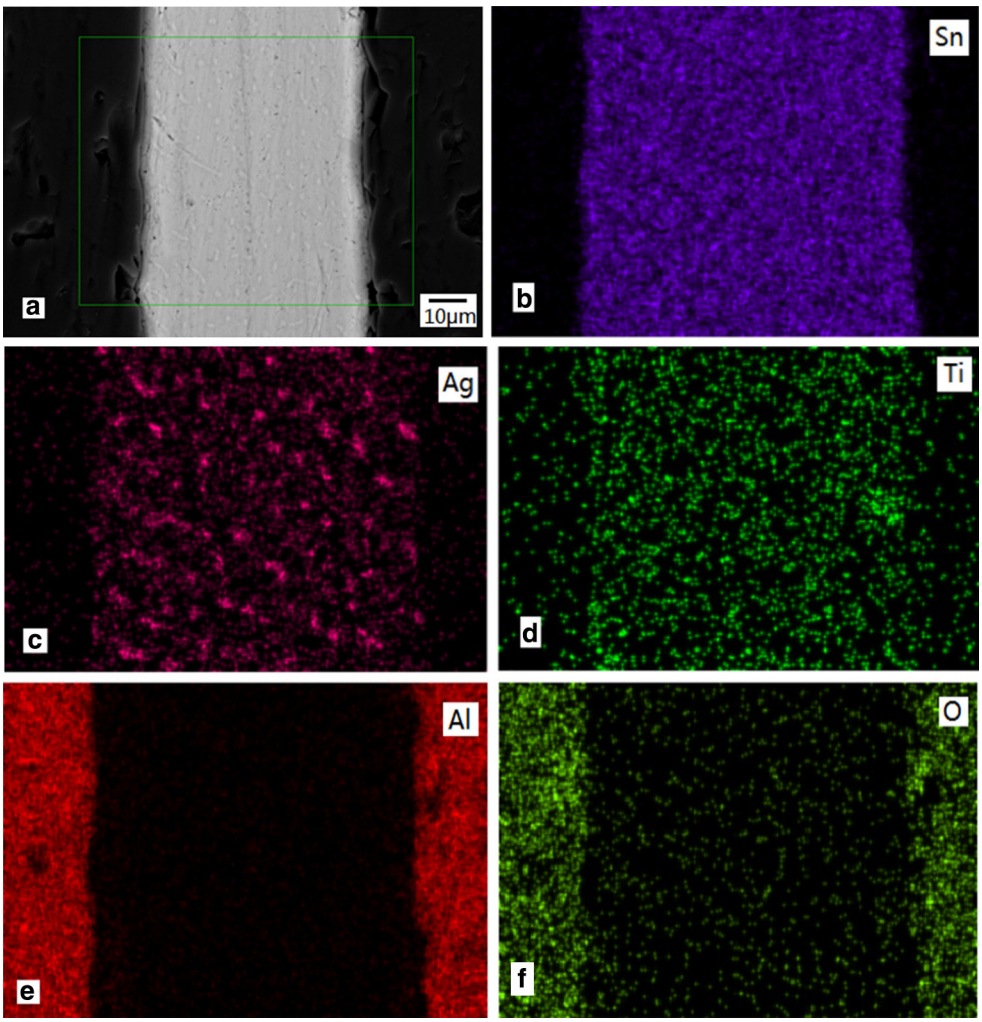

Fig. 6 Micrograph and element maps for Al_2O_3/Sn3.5Ag4Ti(Ce,Ga)/Al_2O_3 joint soldered at 250 °C for 1 h **a** micrograph; **b** map of tin; **c** map of silver; **d** map of titanium; **e** map of aluminum; **f** map of oxygen

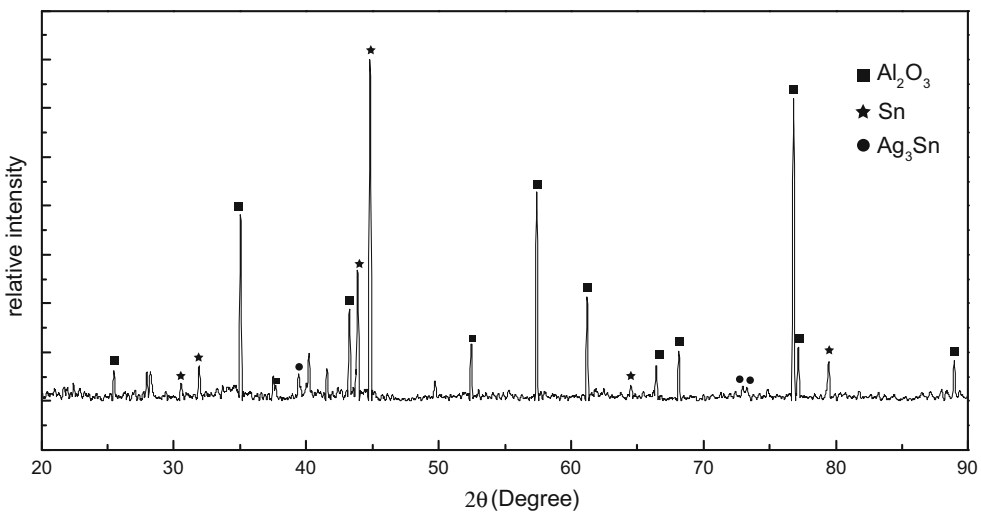

Fig. 7 X-ray diffraction performed on the bonding surface after mechanical separation at the alumina/active solder interface

Table 2 Thermodynamic data for the reaction $Al_2O_3(s) + 3Ti(l) = 3TiO(s) + 2Al(l)$ [15]

T(K)	ΔH(J mol^{-1})	ΔG(J mol^{-1})	ΔS(J K^{-1})	K_{eqm}
1073	41,980	4971	34	0.572
1173	45,291	1374	37	0.886
1209.20	46,546	0.1	35	0.9999
1209.21	46,546	0	35	1.0000
1209.22	46,547	−0.6	35	1.0001
1273	48,826	−2514	40	1.2682
1373	52,562	−6689	43	1.7967
1473	55,862	−11,140	45	2.483
1573	55,416	−15,671	45	3.3143

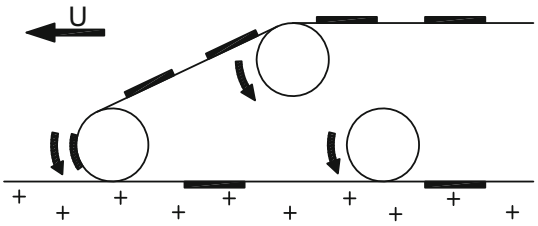

Fig. 8 A model of how the active atoms move to the liquid–solid interface is similar to the motion of a caterpillar vehicle, U is the liquid spreading direction (Dussan–Davis movement)

In the present study, it might be impossible to take chemical reaction between alumina and active solder in terms of thermodynamics. Ti will be adsorbed on the surface of alumina substrate. In our observation, titanium is not found to obviously segregate at the alumina/active solder interface after soldering at 250 °C for 15 min. It may be due to the Ti migration and chemical adsorption is a slow process and the time of 15 min is not long enough for titanium to obviously segregate. When the soldering time increases to 30 min, the titanium element can be observed to obviously segregate at the alumina/active solder interface.

With the increase in soldering time, the segregated active atoms at solid–liquid interface may diffuse into the liquid again due to the concentration difference between the interface and liquid inside. The segregation of titanium at interface is gradually becoming not obvious. This may be the reason why the titanium element almost uniformly distributes after soldering at 250 °C for 60 min. It might be also indicated that the active atoms at the solid–liquid interface could be monolayer adsorption, but not the multilayer adsorption, and the apparent on multilayer adsorption phenomenon is a transient process.

3.3 The estimation of absorbability

To understand the segregation phenomena of Ti in soldering process, it is necessary to analyze the adsorbability of the Ti atoms at the solid–liquid interface. According to the model of Weyl [20], due to the larger size and polarizability of oxygen atoms than metal atoms, a few atomic layers in close to the surface of the oxide ceramic may result in the occurrence of structure relaxation which make the larger oxygen ions closely occupy the outermost surface of the ceramic, and force the metal ions move to the internal. When titanium atoms arrive at the interface of alumina, maybe the titanium atoms and oxygen atoms in alumina exchange electron to form ion covalent bonds and complete the chemical adsorption.

According to the adsorption force calculation by Li [21, 22], the work of adhesion W can be expressed as:

$$W = S_W \times n_{ws} \tag{3}$$

where S_w is the slope parameter of the work of adhesion, and n_{ws} is the electron density at the boundary of the Wigner–Seitz cell of the metals. The slope parameter S_w of Al_2O_3 is about 266 mJ m^{-2} du^{-1}, and the electron density n_{ws} of Ti is 3.51 du [23]. The du is the density unit, and 1 du = 6 × 10^{22} electrons cm^{-3}. Hence,

$$W = 266\,\text{mJ}\,\text{m}^{-2}\,\text{du}^{-1} \times 3.51\,\text{du} = 933.66\,\text{mJ}\,\text{m}^{-2} \tag{4}$$

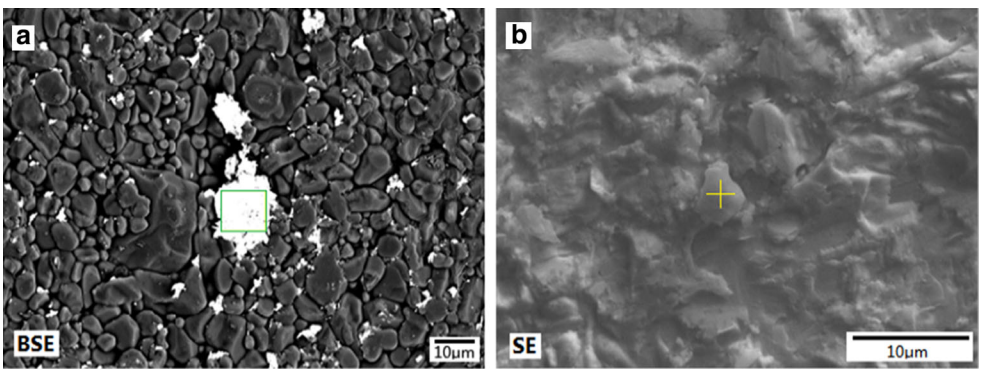

Fig. 9 Fractographs of Al_2O_3/Al_2O_3 joint with Sn3.5Ag4Ti(Ce,Ga) active solder after shear testing. **a** The Al_2O_3 side; **b** the active solder side

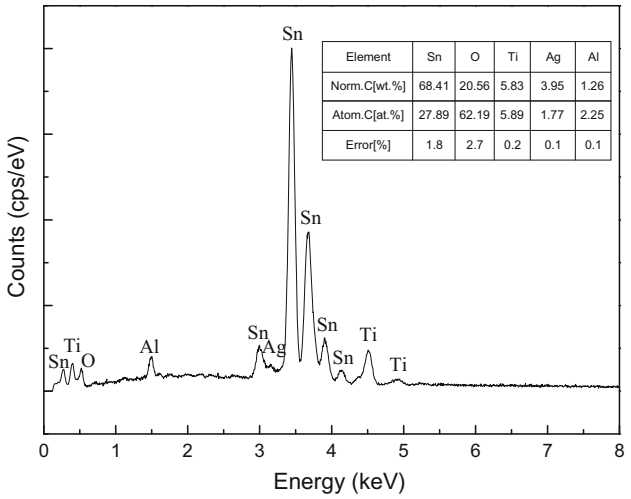

Fig. 10 EDS spectrum of the solder remained in the alumina side

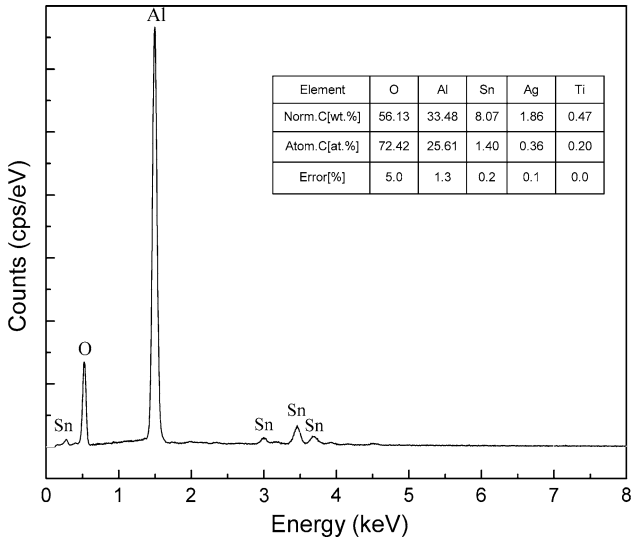

Fig. 11 EDS spectrum of the alumina particle remained in the solder side

It is indicated that the attraction of the alumina surface to the titanium atoms exists to attract the titanium atoms to move to the interface. It is this attraction force leading to the Ti atoms segregating at the solid–liquid interface.

4 Shear strength of solder joints

Shear test results show that fracture of all samples occurs at the active solder/alumina interface. Fractographs of Al_2O_3/Al_2O_3 joint after shear testing for the specimen bonded at 250 °C for 60 min are shown in Fig. 9. The microstructures of the alumina and active solder side are shown in Fig. 9a, b respectively. SEM micrographs show that some of solder is remained at the alumina side, and some of the alumina particles are remained in the solder side. This might be indicated that the soldering strength is strong enough due to the chemical adsorption and the formation of ion covalent bonds. The residuals on the fracture surfaces in each side were analyzed by EDS. Figure 10 shows the EDS spectrum of the solder remained in the alumina side. It can be found that relative titanium concentration of 5.83 wt% at the interface is obviously higher than the content of titanium in the solder, which may further confirm that titanium segregates at the alumina/active solder interface. Figure 11 shows the EDS spectrum of the alumina particle remained in the solder side. It is obvious that the relative aluminum and oxygen concentration is high, which indicates that there are some alumina particles remained in the solder side (Fig. 12).

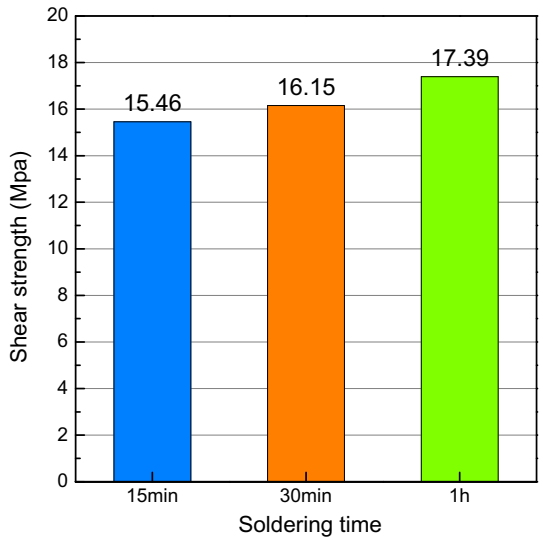

Fig. 12 Shear strength of Al_2O_3/Al_2O_3 joints with soldering time of 15 min, 30 min, 1 h

The average shear strength is measured to be 15.46, 16.15, and 17.39 MPa for the samples with soldering times of 15, 30, and 60 min respectively. Results indicate that joint strength slightly increases with the increase in soldering time. The high enough joint strength might be because the titanium atoms and oxygen atoms at the interface exchange electron to form ion covalent bonds and complete the chemical adsorption. The shear strength meeting the standard requirements of die bonding application in the MIL-STD-883G-2006 demonstrates that the alloy filler could be used to attach semiconductor die or surface mounted passive elements to package headers or other substrates.

5 Conclusions

Sn3.5Ag4Ti(Ce,Ga) active alloy filler was used for joining alumina with alumina at low temperature in air in this study. The microstructure of the interface and the titanium distribution were characterized. The bonding strengths were measured and the shear fracture microstructure was analyzed. The main conclusions are summarized as bellow:

1. Titanium element is not found to obviously segregate at the alumina/active solder interface for the samples soldering at 250 °C for 15 min, but cluster together inside of the Sn3.5Ag4Ti(Ce,Ga) filler metal. When the soldering time increased to 30 min, titanium element is found to obviously segregate at the alumina/active solder interface. Once the soldering time increase to 60 min, titanium element almost uniformly distributed in the joints.
2. Results might present the fact that a comprehensive analysis of chemical adsorption kinetics between titanium and alumina should divide the soldering process into its constituent steps as follows: (a) the repulsive force between the atoms in the liquid solder causes a part of active elements to move to the liquid surface and the solid–liquid interface; (b) due to the chemical adsorption and migration for a relative long time, a temporary stack of active atoms at the interface occurs; (c) with the increase in soldering time in soldering process, the segregated active atoms at solid–liquid interface diffuse into the liquid again due to the concentration gradient.
3. The Sn3.5Ag4Ti(Ce,Ga) alloy filler can wet the alumina well under the agitation of external force. The joint strength slightly increases with the increase in soldering time. The shear strength is measured to be 15.46, 16.15, and 17.39 MPa for the samples with soldering time of 15, 30, and 60 min respectively. No continuous reaction products could be detected at the solder-alumina interface by SEM and XRD. These observations indicate that there may be a chemical adsorption to form the joint in soldering dynamic process at the interface without chemical reaction. Theoretical analysis result shows that the adsorption work between alumina and Ti element is about 933.66 mJ m^{-2}, which further confirms that the adsorption force exists between the alumina surface and the titanium atoms to form the strong enough joint.

Acknowledgments This research is supported by the Planned Science and Technology Project of Guangdong Province, China (No. 2013B010403003) and the Opening Project of Science and Technology on Reliability Physics and Application Technology of Electronic Component Laboratory (No. ZHD201305).

References

1. R. Mayappan et al., J. Mater. Sci. Mater. Electron. **25**, 2913–2922 (2014)
2. L.C. Tsao, J. Mater. Sci. Mater. Electron. **25**, 233–243 (2014)
3. O.M. Akselsen, J. Mater. Sci. **27**, 1989–2000 (1992)
4. T.H. Chuang, M.S. Yeh, Y.H. Chai, Metall. Mater. Trans. A **31**, 1591–1597 (2000)
5. M.G. Nicholas, T.M. Valentine, M.J. Waite, J. Mater. Sci. **15**, 2197–2206 (1980)
6. T. Laurila, V. Vuorinen, M. Paulasto-Kröckel, Mater. Sci. Eng. R **68**, 1–38 (2010)
7. J.J. Stephens, F.M. Hosking, T.J. Headley, Metall. Mater. Trans. A **34A**, 2963–2972 (2003)
8. D. Sciti, A. Bellosi, L. Esposito, J. Eur. Ceram. Soc. **21**, 45–52 (2001)
9. L. Rongti et al., Mater. Sci. Eng. A **335**, 21–25 (2002)
10. S.Y. Chang, T.H. Chuang, C.L. Yang, J. Electron. Mater. **36**, 1193–1198 (2007)
11. R. Koleňák et al., Mater. Des. **32**, 3997–4003 (2011)
12. Y.S. Chung, T. Iseki, Eng. Fract. Mech. **40**, 941–949 (1991)
13. L. Gremillard et al., J. Mater. Res. **21**, 3222–3233 (2006)
14. S. Kalogeropoulou, C. Rado, N. Eustathopoulos, Scr Mater. **41**, 723–728 (1999)
15. Abhijit Kar et al., J. Mater. Sci. **42**, 5556–5561 (2007)
16. L. Gremillard, E. Saiz, J. Chevalier, Z. Metallkd. **95**, 261–265 (2004)
17. A. P. Xian, PhD Dissertation, Institute of Metal Research Chinese Academy of Sciences (1991)
18. Ai-Ping Xian, J. Mater. Sci. **28**, 1019–1030 (1993)
19. P.G. de Gennes, Rev. Mod. Phys. **57**, 827–863 (1985)
20. W.A. Weyl, Ceramic Age **65**, 28 (1952)
21. J.-G. Li, Mater. Lett. **22**, 169–174 (1995)
22. J.-G. Li, Mater. Chem. Phys. **47**, 126–145 (1997)
23. B.W. Zhang, W.Y. Hu, X.L. Shu, *Theory of Embedded Atom Method and its Application to Materials Science*, 1st edn. (Hunan University Press, Changsha, 2003), p. 8